2008 IEEE International Conference on
Robotics and Automation
Pasadena, CA, USA, May 19-23, 2008

# On the Embodiment That Enables Passive Dynamic Bipedal Running

Dai Owaki, Koichi Osuka and Akio Ishiguro

*Abstract*— **The control and mechanical systems of an embodied agent should be tightly coupled so as to emerge useful functionalities such as adaptivity. This indicates that the mechanical system as well as the control system should be responsible for a certain amount of "computation" for generating the behavior. However, there still leaves much to be understood about to what extent "computational offloading" from the control system to the mechanical system should be achieved. In order to effectively consider this, here we particularly focus on a passive dynamic running biped whose behavior is generated purely from its mechanical system, and investigate how the body's properties influence the resulting behavior. Through the numerical simulations, we have found that two elastic parameters of its body, leg spring constant and hip coil spring constant, play a crucial role, and depending on which various kinds of stable gait patterns are generated. To the best of our knowledge, this has not been explicitly addressed so far. The results obtained are expected to shed a new light on to what extent the mechanical system should be responsible for generating the behavior.**

## I. INTRODUCTION

The behavior of an embodied agent is generated through the tight interaction between its control system (*i.e.* brain), mechanical system (*i.e.* body), and the environment[1][2]. Considering the fact that the control and mechanical systems, which are normally the targets to be designed for robotic agents, are positioned at the source of this interaction, these two systems should be treated with an equal emphasis. This strongly suggests that a certain amount of computation for generating the behavior should be *offloaded* from the control system to its mechanical system. In order to explicitly indicate this kind of "embodied" computation to be embedded in the mechanical system, Pfeifer *et al.* have recently coined the term called *morphological computation*[3] which is expected to be an indispensable concept for building adaptive agents. Despite its appealing concept, there still leaves much to be understood about how such "computational offloading" can be achieved so as to emerge useful functionalities such as adaptivity.

In light of these facts, this study is intended to deal with the following questions:

- To what extent computational offloading from the control system to the mechanical system should be done?
- What sort of the body's properties should be focused on so as to effectively exploit the morphological computation?

D. Owaki and A. Ishiguro are with the Department of Electrical and Communication Engineering, Tohoku University, Sendai, Japan {owaki@cmplx./ishiguro@}ecei.tohoku.ac.jp
K. Osuka is with the Department of Mechanical Engineering, Kobe University, Kobe, Japan osuka@mech.kobe-u.ac.jp

Since this research field is still in its infancy, it is of great worth to accumulate various case studies at present. In order to intensively investigate the questions above, here we have particularly focused on the "elasticity" of the body, and show how the computational offloading derived from this property is exploited to generate diverse behaviors.

To this end, we have focused on *passive dynamic bipedal running*. The reasons why we have taken this phenomenon are threefold: first, since passive dynamic locomotion is generated purely from its mechanical system, we can intensively investigate the mechanism of morphological computation; second, since the seminal works of McGeer[4], passive dynamic walking has been attracted lots of concerns, and so far various interesting knowledge, *e.g.*, doubling bifurcation phenomena, have been accumulated[5][6]. In contrast to this, still few studies have been done concerning passive dynamic running[7]; third, the body's intrinsic dynamics becomes increasingly dominant in rapid locomotion[8]. This allows us to expect that the amount of morphological computation to be exploited relatively increases in running compared to walking.

We have modeled a passive dynamic running biped in a numerical simulator, and have investigated how the body properties influence the resulting behavior. As a result, very interestingly, we have found that two elastic parameters of its body —leg spring constant and hip coil spring constant— play a crucial role, and depending on which various kinds of stable gait patterns such as running, walking, skipping, and the mixture of these gait patterns appear. This is an unexpected result. To the best of our knowledge, this phenomenon has not yet been explicitly addressed so far. The results obtained are expected to shed a new light on to what extent the mechanical systems should be responsible for generating the behavior.

This paper is organized as follows: Section II briefly reviews the previous and related work. Section III explains the passive dynamic running biped model. Section IV then discusses simulation data and section V presents conclusions and the projected work.

## II. PREVIOUS AND RELATED WORK

This section briefly introduces several prior studies related to bipedal running. McGeer showed the possibility of passive dynamic bipedal running in numerical experiments, employing a simple compass-like biped with linear springs[7]. In contrast to passive dynamic *walking*, few appear to have dealt with passive dynamic *running*[9].

On the other hand, several studies on the analysis of running have been already reported. Seyfarth *et al.* analyzed

TABLE I
PARAMETERS FOR BIPED

| | | |
|---|---|---|
| $m_{hip}$ | [kg] | Hip mass |
| $m_{leg}$ | [kg] | Leg mass |
| $l$ | [m] | Leg length |
| $r_g$ | [m] | Relative distance between hip mass and leg mass |
| $r_f$ | [m] | Relative distance between leg and leg mass |
| $k_{leg}$ | [N/m] | Spring constant of legs (linear spring) |
| $c_{leg}$ | [Ns/m] | Damping constant of legs |
| $k_{hip}$ | [Nm/rad] | Spring constant of hip joint (coil spring) |
| $c_{hip}$ | [Nms/rad] | Damping constant of hip joint |

the motion of running with a spring–mass model[10], clearly showing that parameters such as the spring constant and the angle of attack play crucial roles in increasing self-stabilization of running motion. Ghigliazza *et al.* adopted a spring-loaded inverted pendulum (SLIP) model and explained that running is made stable by a simple control algorithm particularly focusing on the angle of attack[11]. In our previous work[12], also, we verified the effect of nonlinearity in the leg elasticity on stability of running and showed a certain type of nonlinearity plays a crucial role in enhancing the stability of running. These works did not, however, treat with purely passive dynamic locomotion because the angle of attack is parameterized and constant at each step and did not consider the importance of swing leg dynamics in bipedal locomotion.

## III. THE METHODS

### A. The Model

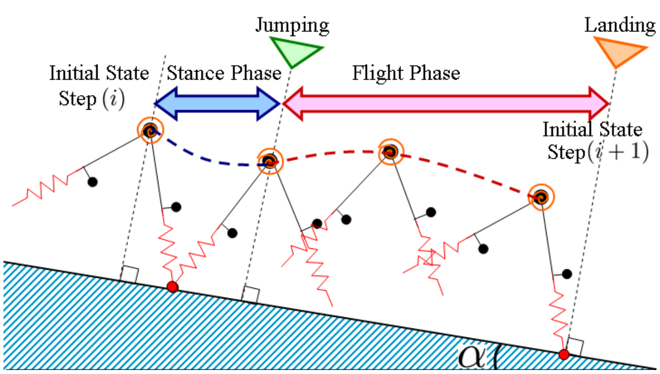


Fig. 1. Running motion through one period. One period starts at touch-down (landing) and ends at next touch-down.

Figure 1 shows the model of a passive dynamic running biped, moving thorough one period of running. We assume that touch-down is the initial state of running. Running is thus described as a periodic alternation between *stance* and *flight* phases, so the equations of motion for passive dynamic bipedal running should be described for each phase. In this study, based on work by McGeer[7], we employ a model of passive dynamic running biped to describe the stance and flight phase. In the sections that follow, we show how we formulate detailed equations of motion for each phase.

### B. Equations of Motion

*1) Stance Phase:* Equations of motion for the stance phase are given by the following equation employing the Euler-Lagrange approach:

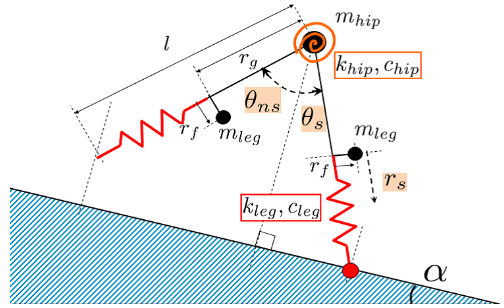


(a) Stance phase: one leg contacts with the ground slope

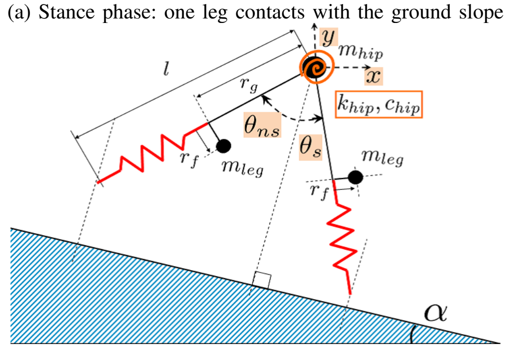


(b) Flight phase: two legs are in the air

Fig. 2. Model of each phase: the distinguishing feature is two elastic elements that implemented to stance leg $k_{leg}$ and to hip joint $k_{hip}$

$$\boldsymbol{M_s}(\boldsymbol{\theta}_s)\ddot{\boldsymbol{\theta}}_s + \boldsymbol{N_s}(\boldsymbol{\theta}_s, \dot{\boldsymbol{\theta}}_s)\dot{\boldsymbol{\theta}}_s + \boldsymbol{g}(\boldsymbol{\theta}_s, \alpha) = \boldsymbol{0}, \quad (1)$$

where $\boldsymbol{M_s}(\boldsymbol{\theta}_s)$ represents the inertia matrix, $\boldsymbol{N_s}(\boldsymbol{\theta}_s, \dot{\boldsymbol{\theta}}_s)$ represents the centrifugal and Coriolis term, and $\boldsymbol{g}(\boldsymbol{\theta}_s, \alpha)$ represents the gravity term. In this paper, we spare someone the details of these matrixes because of space limitations. $\boldsymbol{\theta}_s = [\theta_{ns}, \theta_s, r_s]^T$ corresponds to the configuration vector for the stance phase. As shown in Fig. 2 (a), $\theta_{ns}$ and $\theta_s$ represent the angle of the stance and swing leg to the slope normal. $r_s$ is the amount of leg shortening. Note that $r_s$ is set to 0 when a leg is at touch-down. We assume that the stance foot remains on the slope and treat as a hinge during the stance phase. The body parameters of a biped are listed in Table I. $\alpha$ denotes the slope angle.

*2) Flight Phase:* Similar to the stance phase, equations of motion for the flight phase are given by the following equation:

$$\boldsymbol{M_f}(\boldsymbol{\theta}_f)\ddot{\boldsymbol{\theta}}_f + \boldsymbol{N_f}(\boldsymbol{\theta}_f, \dot{\boldsymbol{\theta}}_f)\dot{\boldsymbol{\theta}}_f + \boldsymbol{g}(\boldsymbol{\theta}_f, \alpha) = \boldsymbol{0}, \quad (2)$$

where $\boldsymbol{M_f}(\boldsymbol{\theta}_f)$ represents the inertia matrix, $\boldsymbol{N_f}(\boldsymbol{\theta}_f, \dot{\boldsymbol{\theta}}_f)$ represents the centrifugal and Coriolis term, and $\boldsymbol{g}(\boldsymbol{\theta}_f)$ represents the gravity term. $\boldsymbol{\theta}_f = [\theta_{ns}, \theta_s, x, y]^T$ corresponds to the configuration vector for the flight phase. As shown in Fig. 2 (b), $\theta_{ns}$ and $\theta_s$ represent the angle of the swing legs to the slope normal. We distinguish between $\theta_{ns}$ and $\theta_s$ by using the state of the stance phase. $x$ and $y$ are the position of the hip mass. The body parameters of a biped are listed in Table I. $\alpha$ denotes the slope angle.

### C. State Transition Rules

As mentioned above, running is described as a series of stance and flight phases. We must thus consider state transition rules between these two phases, allowing us to correlate phase variables consistently. To this end, we define the state transition rules at the point of *jumping* and of *landing*, summarized as follows: linear and angular momentums and energy are conserved at *jumping*; and whereas energy dissipation occurs at *landing* due to the foot colliding with the slope. In the following, we explain how we formulate the events of jumping and of landing.

*1) Jumping:* Jumping occurs when the following equations are satisfied:

$$r_s^- \quad = 0. \tag{3}$$

Because linear and angular momentum and energy just before and after the jumping are conserved, the state transition rules at jumping are given by

$$\boldsymbol{x}_f^+ = \begin{bmatrix} \theta_{ns}^+ \\ \theta_s^+ \\ x^+ \\ y^+ \\ \dot{\theta}_{ns}^+ \\ \dot{\theta}_s^+ \\ \dot{x}^+ \\ \dot{y}^+ \end{bmatrix} = \begin{bmatrix} \theta_{ns}^- \\ \theta_s^- \\ l\sin(\theta_s^- + \alpha) + x_{s0} \\ l\cos(\theta_s^- + \alpha) + y_{s0} \\ \dot{\theta}_{ns}^- \\ \dot{\theta}_s^- \\ l\cos(\theta_s^- + \alpha)\dot{\theta}_s^- - \sin(\theta_s^- + \alpha)\dot{r}_s \\ -l\sin(\theta_s^- + \alpha)\dot{\theta}_s^- - \cos(\theta_s^- + \alpha)\dot{r}_s \end{bmatrix}, \tag{4}$$

where $\boldsymbol{x}_f = [\boldsymbol{\theta}_f, \dot{\boldsymbol{\theta}}_f]^T$. $[\theta_{ns}^-, \theta_s^-, r_s^-, \dot{\theta}_{ns}^-, \dot{\theta}_s^-, \dot{r}_s^-]^T$ and $[\theta_{ns}^+, \theta_s^+, x^+, y^+, \dot{\theta}_{ns}^+, \dot{\theta}_s^+, \dot{x}^+, \dot{y}^+]^T$ represent state variables just before and after the jumping, respectively. $x_{s0}$ and $y_{s0}$ correspond to the position of the stance foot just before the jumping.

*2) Landing:* Landing occurs when the following equation is satisfied:

$$y^- = l\cos(\theta_{ns}^- + \alpha) - \tan(\alpha)(x^- - x_{s0}) + y_{s0}, \tag{5}$$

where $x_{s0}$ and $y_{s0}$ correspond to the position of the stance foot just before the jumping. Since linear and angular momentums just before and after the landing is conserved, the state transition rules at landing are expressed as:

$$\boldsymbol{x}_s^+ = \boldsymbol{R}(\boldsymbol{x}_f^-) = \begin{bmatrix} \boldsymbol{T}_r\boldsymbol{\theta}_f^- & \boldsymbol{0} \\ \boldsymbol{0} & (\boldsymbol{P}_s)^{-1}\boldsymbol{P}_f\dot{\boldsymbol{\theta}}_f^- \end{bmatrix} \tag{6}$$

$$\boldsymbol{T}_r = \begin{bmatrix} 0 & 1 & 0 & 0 \\ 1 & 0 & 0 & 0 \\ 0 & 0 & 0 & 0 \end{bmatrix} \tag{7}$$

where $\boldsymbol{x}_s = [\boldsymbol{\theta}_s, \dot{\boldsymbol{\theta}}_s]^T$. $\boldsymbol{x}_f^-$ and $\boldsymbol{x}_s^+$ represent state vectors just before and after the landing, respectively. The matrix $\boldsymbol{P}_s$ and $\boldsymbol{P}_f$ are derived by employing the conservation of linear momentum parallel to the stance leg and of angular momentum around foot contact point and hip joint:

$$\boldsymbol{P}_s\dot{\boldsymbol{\theta}}_s^+ = \boldsymbol{P}_f\dot{\boldsymbol{\theta}}_f^-, \tag{8}$$

In this paper, we spare someone the details of these matrixes because of space limitations. In sum, the state transition rules are summarized as follows:

$$\begin{array}{c} \text{Initial state at step } (i)\text{: } (\boldsymbol{x}_s^0)_i \\ \Downarrow \\ \text{Stance phase: } \boldsymbol{x}_s \\ \Downarrow \\ \text{Jumping: } \boldsymbol{x}_s^- \mapsto \boldsymbol{x}_f^+ \\ \Downarrow \\ \text{Flight phase: } \boldsymbol{x}_f \\ \Downarrow \\ \text{Landing: } \boldsymbol{x}_f^- \mapsto \boldsymbol{x}_s^+ \\ \Downarrow \\ \text{Initial state at step } (i+1)\text{: } (\boldsymbol{x}_s^0)_{i+1}, \end{array}$$

where $(\boldsymbol{x}_s^0)_i$ and $(\boldsymbol{x}_s^0)_{i+1}$ are the initial state for the stance phase at step $(i)$ and $(i+1)$, respectively. If landing foot (angle of attack is $\theta_{ns}$) replaces to the other foot (angle of attack is $\theta_s$), the state variable $\theta_{ns}$ replaces to $\theta_s$ in the noted above equations (5)–(8) (This occurs in skipping gaits like Fig. 6). If landing from stance to stance occurs before jumping, biped performs walking like Fig. 4, 5 (transition rule is modeled similar to landing from flight to stance). Note that state transition from one phase to another phase occurs depending on the physical condition of the biped.

## IV. SIMULATION RESULTS

### A. Verification of Elastic Elements' Effect on Gait Pattern

In order to determine the effect of body dynamics properties, particularly elastic elements, on behaviors that generated by a biped, we observed gait pattern, implementing a linear spring $K_{leg} = k_{leg}/(m_{hip}l^2) = 750 \sim 4000$ into the leg and a coil spring $K_{hip} = k_{hip}/(m_{hip}l^2) = 5.0 \sim 100.0$ into the hip joint. Figure 3–6 compares gait patterns performed by the biped with different embodiments (the accompany video shows these gait patterns). These motions represent steady–state patterns. The upper figures show the snapshots per 0.05[s]. In these figures, red lines represent trajectories of hip mass. The second graphs from the top represent gait diagrams for the biped. In these graphs, red and green color areas show stance phases of right and left legs. The third graphs from the top show Ground Reaction Force (hereafter GRF) perpendicular and parallel to the slope. The lower graphs show Froude number $F_r$ defined on stance phase (see Appendix). Note that the biped performs different gait patterns, depending on the only two elastic parameters, that is, leg spring constant $K_{leg}$ and coil spring constant $K_{hip}$. Other body parameters were set as follows: $l = 0.30$, $m_{hip} = 10.0$, $C_{leg} = 9.00$, $C_{hip} = 0.00, \xi = m_{leg}/m_{hip} = 0.200$, $\eta = r_g/l = 0.50$, $r_f = 0.00$, and $\alpha = 0.070$[rad]. In this paper, we distinguished between gait patterns by employing (i) gait diagram, (ii) GRF, (iii) Froude number in Fig. 3–6. In what follows, we explain each gait pattern in detail.

*1) Running gait:* The reason why we regard gait 1 $(K_{leg}, K_{hip}) = (1250, 25)$ as running is threefolds: (1) the biped performs flight phase period in 0.024[s]; (2) this biped demonstrates one peak curve of GFR perpendicular to the slope during one period; (3) $F_r > 1$. One of fascinating aspects of this result is that this profile gives well agreement with that human performs in running[13]. Moreover, running speed performed by this biped corresponds to 2.30[m/s].

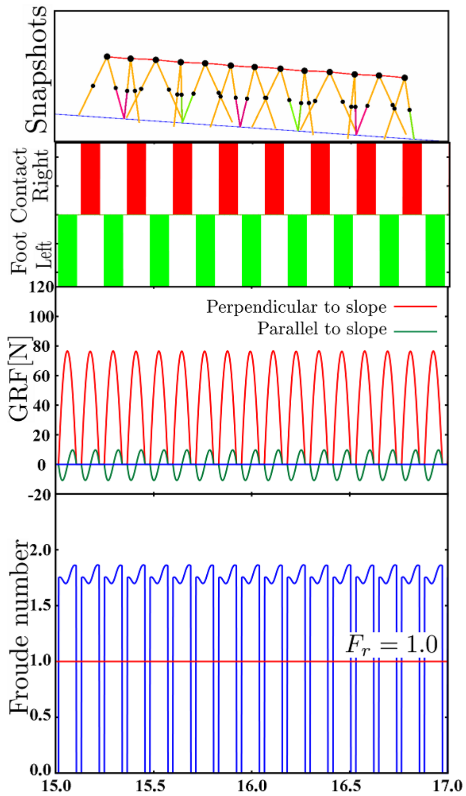


Fig. 3. Gait 1: Running with $K_{leg} = 1250, K_{hip} = 25$. Note that GFR perpendicular to the slope becomes one peak curve during one period and Froude number thoroughly greater than 1.

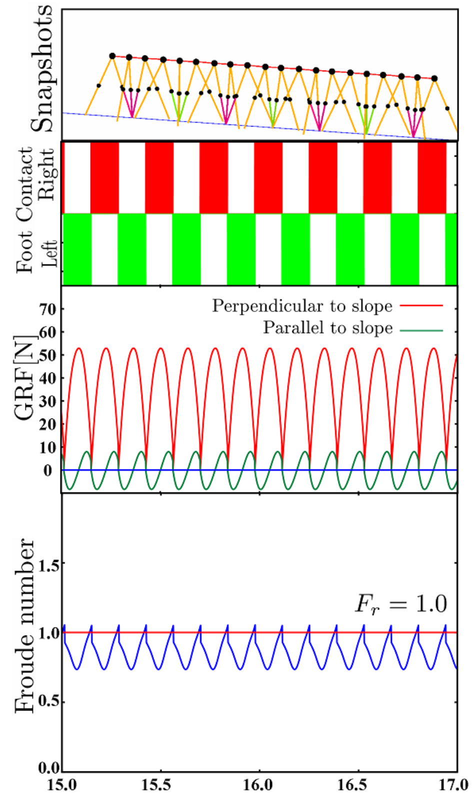


Fig. 4. Gait 2: 1-peak-GRF walking with $K_{leg} = 750, K_{hip} = 25$. Note that GFR perpendicular to the slope becomes one peak curve during one period.

2) *Walking gait:* Interestingly, our model shows walking gaits like gait 2 and 3 (Fig. 4 and 5), in which biped cannot perform flight phase period at all and Froude number $F_r$ is less than 1. Furthermore, the gait 2 shows one peak curve of GFR perpendicular to the slope during one period, whereas the gait 3 shows two peaks curve of that. Therefore, we define the former as *1-peak-GRF walking* gait and the latter as *2-peak-GRF walking* gait. Walking speed of the gait 2 and 3 corresponds to 1.56 and 0.687[m/s]. Similar to running (the gait 1), these results correspond to the profiles that human performs in walking. In addition to this, it is highly interesting that the GRF curve vary depending on walking speed like human walking[13].

3) *Skipping gait:* Gait 4 (Fig. 6) is another unexpected results obtained in this paper. We regard this gait as *skipping* because this gait diagram shows that switching stance leg occurs every two steps. The profile of this gait is similar to that of the gait 3 (walking that performs two peaks GRF). Locomotion speed of this gait corresponds to 0.875[m/s].

One of fascinating aspects of these results is that passive dynamic gait patterns is generated from the results of time evolution toward the most dynamically stable state, that is, morphological computation and these behaviors that generated from passive dynamics are well agreement with the behaviors that human performs from the viewpoint of GRF, velocity and so on[13]. In the sections that follow, we discuss the contributing factor that determines bipedal gait patterns.

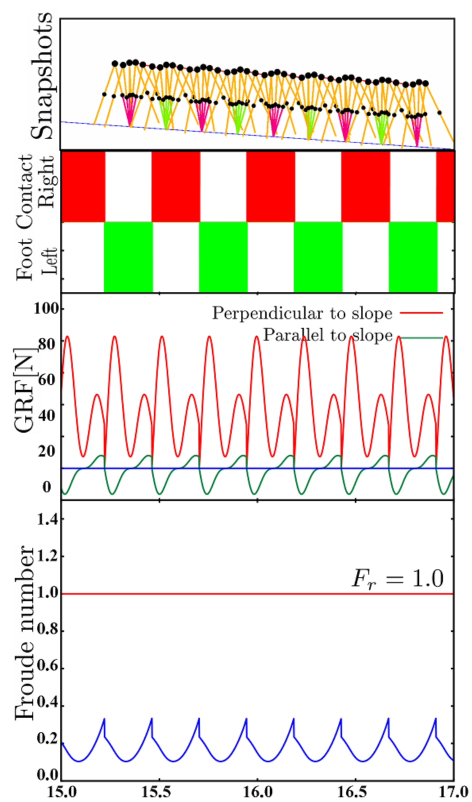


Fig. 5. Gait 3: 2-peak-GRF walking with $K_{leg} = 2000, K_{hip} = 8$. Note that GFR perpendicular to the slope becomes two peaks curve during one period.

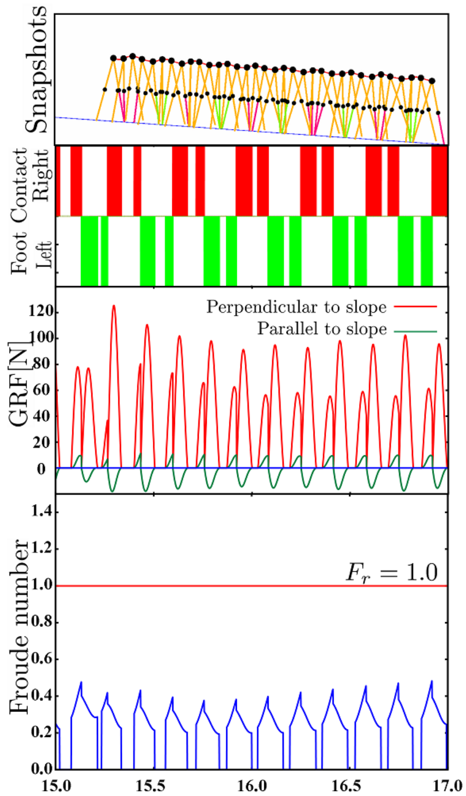


Fig. 6. Gait 4: Skipping with $K_{leg} = 4000, K_{hip} = 18$. Note that the stance leg switches every two steps.

## B. Contributing Factor for Gait Patterns

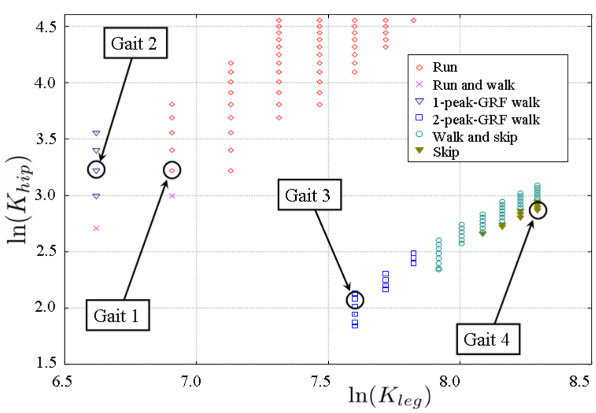


Fig. 7. Distribution of gait patterns in $\ln(K_{leg})$–$\ln(K_{hip})$. Circles indicate the gait 1–4 shown in figure 3–6. Note that $K_{leg}$ and $K_{hip}$ explicitly correlate with gait patterns.

Figure 7 shows the distribution of gait patterns in paramater space $\ln(K_{leg})$–$\ln(K_{hip})$. Gait 1–4 in this figure correspond to those in Fig. 3–6. Each plotted point represents each parameter set $(K_{leg}, K_{hip})$ that exhibits steady-state pattern. In addition to the gait patterns in Fig. 3–6, the mixture of 1-peak-GRF walking and running, or 2-peak-waking and skipping appear as shown in this figure. This result indicates that two elastic parameters $(K_{leg}, K_{hip})$ explicitly correlate with gait patterns that biped performs. Based on this, we assume a control parameter that defines gait pattern as following equation:

$$C_{gait} = \frac{\ln(K_{hip})}{\ln(K_{leg})} \tag{9}$$

In this paper, we observed the effect of the control parameter $C_{gait}$ on stability of each gait by using Lyapunov exponent, which quantitatively characterizes stability of a system. Figure 8 shows the Lyapunov exponent for each $C_{gait}$. This graph provided us the following three points that have to be noted: first, $C_{gait}$ explicitly correlates with gait pattern ($C_{gait}$–gait); second, each gait (e.g., walking, running) correlates with the value of Lyapunov exponent $\lambda$ (gait–$\lambda$); and finally, running is the most stable gait, the next is walking and after the next is skipping.

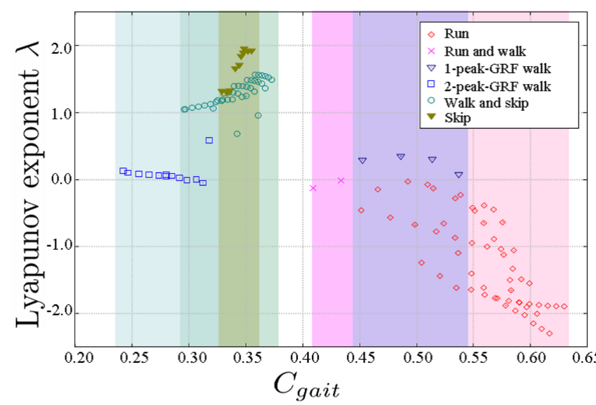


Fig. 8. Stability for various gait patterns. The horizontal axis represents a control parameter $C_{gait}$ and the vertical axis represents Lyapunov exponent. Interestingly, running is the most stable of gait patterns.

In order to consider the contributing factor for gait patterns, we focus on mechanical feedback that structured by its mechanical system. Mechanical feedback, which is determined by elastic elements of its body, significantly influences generating behaviors in locomotion by exploiting passive dynamics of their body. The simple analogue of mechanical feedbacks expressed as $K_{hip}\Delta\theta_{hip}$ and $K_{leg}\Delta r_s$ helps us to perceive these diverse gait patterns ($\Delta\theta_{hip}$ and $\Delta r_s$ represent the deviations of $\theta_{hip} = \theta_{ns} - \theta_s$ and $r_s$ from equilibrium state). Moreover, $K_{hip}$ and $K_{leg}$ determine time constants of their mechanical feedbacks that specifies Froude number by calculating locomotion velocity and stance phase period in locomotion, respectively: (1) Froude number is stemmed from the relative velocity of swing leg to stance leg, depending on the time constant of $K_{hip}\Delta\theta_{hip}$; and (2) stance phase period is stemmed from the interaction time between stance leg and ground slope, depending on the time constant of $K_{leg}\Delta r_s$. The time scale difference of these mechanical feedbacks significantly influences the diverse gait patterns by changing elasticity in the hip joint and legs.

In this paper, we didn't discuss the effect of other parameter on gait patterns, e.g., leg length $l$, the ratio $\xi$ of leg mass $m_{leg}$ to hip mass $m_{hip}$. The leg length determines the swing period of legs as pendulums and leg and hip mass determine the inertia moment of legs. Therefore, these parameters could influence the locomotion velocity and so the Froude number. Based on the above, however, we could conclude that two kinds of time constant of mechanical feedback, which are structured by body elastic parameters, explain diverse gait patterns that biped performs.

## V. CONCLUSIONS AND PROJECTED WORK

In this paper, we have investigated the effect of the body dynamics properties on resulting behavior, employing a passive dynamic running biped whose behavior is generated purely from its mechanical system. Through the numerical simulations, we have found that two elastic parameters, leg spring constant and hip coil spring constant, play a crucial role, and depending on which various kinds of stable gait patterns are generated such as running, walking, skipping, and the mixture of these gait patterns appear. Insofar as we know, this has not been explicitly discussed thus far. The fascinating point of our results is that passive dynamic gait patterns are generated from the results of time evolution toward the most dynamically stable state and these behaviors that generated from passive dynamics are well agreement with the behaviors that human perform. Moreover, we have defined a gait control parameter $C_{gait}$ and have verified the correlation between this parameter and stability of each gait. And finally, we have discussed the contributing factor for gait patterns from view point of time constant of their mechanical feedback that structured by body elasticity. These results strongly suggest that "elasticity" of the body plays an essential role in "morphological computation" or "computational offloading" from the control system to the mechanical systems.

Projected research targets three goals:

1) Stability analysis with an approximate analytical Poincaré map.
2) Gait transition by changing the elasticity of the robot's body adaptively according to the situation encountered.
3) How the control systems should make a contribution to generate diverse behavior in addition to passive dynamics stemming from the mechanical systems.

There still leaves much to be understood about how well-balanced coupling between control and mechanical systems can be achieved, but our results should shed welcome light on these points. Given this, we are expecting to gain deeper insight into what well-balanced coupling is and should be.

## ACKNOWLEDGMENTS

This work was supported in part by a Grant-in-Aid for Scientific Research on Priority Areas "Emergence of Adaptive Motor Function through Interaction between Body, Brain and Environment" and by Tohoku Neuroscience Global COE Basic & Translational Research Center for Global Brain Science from the Japanese Ministry of Education, Culture, Sports, Science and Technology.

## APPENDIX

The dimensionless Froude number quantitatively distinguishes between walking and running by employing locomotion velocity: if the Froude number is larger than 1, jumping off the ground is achieved[13]. The Froude number is defined as the ratio of the inertial force applied to the mass center to the gravitational force to the leg direction (Fig. 9):

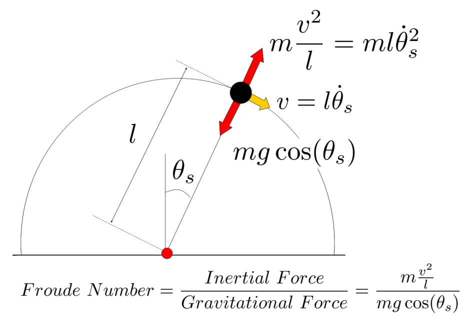


Fig. 9. Froude Number is expressed as the ratio of the inertial force applied to the mass center to the gravitational force to the leg direction.

$$F_r = \frac{m\frac{v^2}{l}}{mg\cos(\theta_s)} = \frac{v^2}{gl\cos(\theta_s)} \leq \frac{v^2}{gl}, \tag{10}$$

where $v$ represents the velocity along the circle trajectory of the mass center, $l$ represents the leg length, and $m$ represents total mass. $\theta_s$ represents the angle of stance leg to the slope normal and $g$ is gravitational acceleration. Thus, jumping off the ground occurs when the following equation is satisfied approximately:

$$F_r \geq 1 \Longrightarrow \frac{v}{\sqrt{gl}} \geq 1. \tag{11}$$

## REFERENCES

[1] R. Pfeifer and C. Scheier, *Understanding Intelligence*, The MIT Press, 1999.
[2] H. Asama, *et al.*, "System Principle on Emergence of Mobiligence and Its Engineering Realization, *in Proc. of the 2003 IEEE/RSJ IROS*, pp.1715–1720, 2003.
[3] R. Pfeifer and F. Iida, *Morphological Computation: Connecting Body, Brain and Environment*, Japanese Scientific Monthly, Vol.58, No.2, pp.48–54, 2005.
[4] T. McGeer, *Passive Dynamic Walking*, The International Journal of Robotics Research, Vol.9, No.2, pp.62–82, 1990.
[5] A. Goswami, B. Thuilot and B. Espau, *A Study of the Passive Gait of a Compass–like biped robot: Symmetry and Chaos*, The International Journal of Robotics Research, Vol.17, No.12, pp.1282–1301, 1998.
[6] M. Garcia, A. Chatterjee, A. Ruina and M. Coleman, *The Simplest Walking Model: Stability, Complexity and Scaling*, ASME Journal of Biomechanical Engineering, Vol. 120, No. 2, pp. 281–288, 1998.
[7] T. McGeer, *Passive Dynamic Running*, in Proc. of the Royal Society of London, Series B, Biological Science, Vol.240, No.1297, pp.107–134, 1990.
[8] R. J. Full and D. E. Koditschek, *Templates and Anchors: Neuromechanical Hypotheses of Legged Locomotion on Land*, The Journal of Experimental Biology, Vol. 202, pp.3325–3332, 1999.
[9] S. – H. Hyon and T. Emura, *Energy-preserving Control of a Passive One-legged Running Robot*, Advanced Robotics, Vol. 18, No. 4, pp. 357–450, 2004.
[10] A. Seyfarth, H. Geyer, M. Gunther, and R. Blickhan, *A Movement Criterion for Running*, Journal of Biomechanics, Vol.35, pp.649–655, 2002.
[11] R. Ghigliazza, R. Altendorfer, P. Holmes, and D. E. Koditschek, *A Simply Stabilized Running Model*, ASME J. on Applied Dynamical Systems, Vol.2, No.2, pp.187–218, 2003.
[12] D. Owaki and A. Ishiguro, *Mechanical Dynamics that Enables Stable Passive Dynamic Bipedal Running –Enhancing Self-Stability by Exploiting Nonlinearity in the Leg Elasticity–* , Journal of Robotics and Macaronis, Vol. 19, No. 4, pp.374–380, 2007.
[13] R. M. Alexander, *Walking and Running*, American Scientist, Vol. 72, pp.348–354, 1984.